

12-2011

# THE DEVELOPMENT OF A FAR RED TO NEAR INFRARED FLUORESCENT PROBE FOR USE IN OPTICAL IMAGING

Margaret Fiedler

Clemson University, [mfiedle@clemson.edu](mailto:mfiedle@clemson.edu)

Follow this and additional works at: [https://tigerprints.clemson.edu/all\\_theses](https://tigerprints.clemson.edu/all_theses)

 Part of the [Materials Science and Engineering Commons](#)

---

## Recommended Citation

Fiedler, Margaret, "THE DEVELOPMENT OF A FAR RED TO NEAR INFRARED FLUORESCENT PROBE FOR USE IN OPTICAL IMAGING" (2011). *All Theses*. 1270.

[https://tigerprints.clemson.edu/all\\_theses/1270](https://tigerprints.clemson.edu/all_theses/1270)

This Thesis is brought to you for free and open access by the Theses at TigerPrints. It has been accepted for inclusion in All Theses by an authorized administrator of TigerPrints. For more information, please contact [kokeefe@clemson.edu](mailto:kokeefe@clemson.edu).

THE DEVELOPMENT OF A FAR RED TO  
NEAR INFRARED FLUORESCENT PROBE  
FOR USE IN OPTICAL IMAGING

---

A Thesis  
Presented to  
The Graduate School of  
Clemson University

---

In Partial Fulfillment  
Of the Requirements for the Degree  
Masters of Science  
Materials Science and Engineering

---

By  
Margaret Lynn Fiedler  
December 2011

---

Accepted by:  
Dr. Stephen Foulger, Committee Chair  
Dr. John Ballato  
Dr. Thompson Mefford

## ABSTRACT

New techniques for biological optical imaging are of great interest for the detection and visualization of processes and disease in both clinical and research areas. One major advancement has been the use of far red and near infrared (NIR) light, as it has the ability to penetrate tissues deeper than other parts of the spectrum which are readily scattered and absorbed by the surroundings. In order to improve the signal to noise ratio and resolution of optical images, contrast agents are used. Fluorescent markers can be modified to attach to specific molecular targets, creating small molecular probes. These targets can be disease sites, or biological molecules which play a major role in processes such as tumor growth. It was our goal to create a new novel fluorescent probe, consisting of a cyanine based far red to NIR marker, and an n-hydroxysuccinimide (NHS) derivative to act as a linker, which could then bind with biological species containing primary amides such as proteins and antibodies, in this model system bovine serum albumin (BSA). The dye, a modified pentamethine carbocyanine, was synthesized according to Shao, et al.,<sup>1</sup> and was chosen for its previous use for *in vivo* visualization and preferred spectral properties, as well as its ability to incorporate different functionalities. The linker was an azide functionalized NHS derivative chosen for its crosslinking ability with species containing primary amides. Azide and alkyne functionality were of great interest due to their reactivity in [2+3] dipolar cycloaddition click type reactions, which was used to attach an azide on the NHS derivative and an alkyne on the dye. This species was then bound to protein, BSA, successfully through this NHS moiety.

## DEDICATION

This work is dedicated to my loving husband, John, who did not hesitate to move 1000 miles away from our friends and families to support my education. John, I could not have survived my time in South Carolina without you! I hope you know how much I appreciate all the love and support you have shown me and continue to show me every day! Also I would like to dedicate this to my family who has been there for me in all of my times of need to give me advice and directions home.

## ACKNOWLEDGMENTS

I would like to thank my advisor, Dr. Stephen Foulger and all of my group members, especially Michael Daniele, for all of their help and advice along the way.

## TABLE OF CONTENTS

	Page
TITLE PAGE .....	i
ABSTRACT .....	ii
DEDICATION .....	iii
ACKNOWLEDGMENTS .....	iv
LIST OF FIGURES .....	vii
LIST OF EQUATIONS .....	ix
CHAPTER	
I. INTRODUCTION .....	1
Background Information .....	1
Motivation .....	4
Research Goals and Approach .....	5
Thesis Outline .....	6
II. LITERATURE REVIEW .....	8
Imaging .....	8
Contrast Agents .....	11
Targeting .....	14
Design of a Molecular Probe .....	16
Spectral Properties .....	17
Cyanine .....	19
Cross linkers .....	21
Proposed Design .....	22
III. EXPERIMENTAL .....	25
Instrumentation and Reagent Information .....	25
Preparation of Dye .....	26
Preparation of Linker .....	32
Click Reaction .....	34
Bioconjugation .....	35

Table of Contents (Continued)

IV.	RESULTS AND DISCUSSION.....	37
	Synthesized Dye.....	37
	Cross linker .....	39
	Assembly of Probe.....	40
	Conjugation to a Protein .....	41
V.	CONCLUSIONS.....	42
VI.	FUTURE WORK.....	43
	REFERENCES.....	45

## LIST OF FIGURES

Figure 1: The optical window is clearly by looking at the absorbance spectra for prevalent biomolecules: water, hemoglobin (Hb), oxygenated hemoglobin (HbO <sub>2</sub> ), and melanin. ....	11
Figure 2: Ultrasound image of a renal carcinoma (denoted with white arrow), with (left) and without (right) the use of microbubbles as a contrast agent. ....	12
Figure 3: A CT scan of the brain with and without contrast agent.....	13
Figure 4: MRI image of a lesion in the skull as shown without (top) and with (bottom).....	14
Figure 5: Composite of 9 optical images of a rat using ICG to map different internal organs non-invasively. ....	15
Figure 6: Cyanine 3, or Cy3, usually absorbs and emits between 500-600nm. ....	20
Figure 7: Cyanine 5, or Cy5, and its derivatives usually absorb between 600-700nm.....	21
Figure 8: Indocyanine Green (ICG), a Cy7 type dye which has been used in the optical imaging field for over 50 years.....	21
Figure 9: N-hydroxysuccinimide (NHS), a cross linker commonly used in the labeling of proteins .....	22
Figure 10: Chemical structure of synthesized molecular probe .....	24
Figure 11: Final dye synthetic route .....	27
Figure 12: Synthetic route for the alkyne intermediate, a reagent in the final dye. ....	28
Figure 13: Synthetic route for the preparation of the indolinium salt intermediate, a reagent in the final dye.....	30



List of Figures (Continued)

Figure 14: The absorbance and emission at 642nm excitation of the unbound dye in water.....	32
Figure 15: Synthesis of the cross linker .....	33
Figure 16: The Huisgen cycloaddition between an alkyne and azide .....	34
Figure 17: The absorbance and emission at 642nm excitation in PBS of the molecular probe when bound to BSA .....	36

## LIST OF EQUATIONS

- Equation 1: Relative quantum yield of an unknown ( $\Phi_x$ ) can be determined through this equation using a well-established standard, where Grad is the slope of the integrated fluorescence intensity vs. the absorbance intensity and  $\eta$  is the refractive index. .... 38
- Equation 2: Beer's law relates the absorbance intensity (A) with the molar absorptivity ( $\epsilon$ ), path length (b=1 cm), and concentration (c). .... 39

## CHAPTER ONE

### INTRODUCTION

#### Background Information

Optical imaging is of great significance to the biological imaging community for its ability to provide high spacial resolution of deep tissues without patient discomfort or the use of ionizing radiation<sup>2</sup>. Imaging is often accompanied by the use of contrast agents which highlight desired areas<sup>3</sup>. There is a particular interest in the development of new targeted contrast agents which are specialized to accumulate at specific sites<sup>4,5</sup>. This provides a better signal to noise ratio and better visualization<sup>2</sup>. It was our goal to investigate and design a new, specialized fluorescent probe which would target proteins or antibodies for use in optical imaging.

Medical imaging is widely relied on for clinical and research purposes, such as the diagnosis of disease and the investigation of biological processes<sup>6,7</sup>. There are several types of imaging, the most popular being ultrasound sonography, x-ray computed tomography (CT scan), magnetic resonance imaging (MRI), and optical imaging. Each has its strengths and weaknesses depending on the area, extent, and precision of visualization required<sup>3,8</sup>.

Ultrasound, as the name implies, uses sound waves which travel through the tissue and the subsequent echoes are recorded<sup>9</sup>. This technique is safe, provides real time

visualization, and instrumentation is portable. However, ultrasound is severely limited by penetration depth, resolution, and by areas which contain air or are surrounded by bone, such as the gastrointestinal tract and the chest cavity<sup>10, 11</sup>. Today, this presents a new problem of imaging the obese population<sup>12</sup>. In addition, soft tissues cannot always be clearly differentiated<sup>9</sup>. CT scans use a series of x-rays around a single axis of rotation and relies on differences in x-ray attenuation, or loss of signal, to differentiate between soft tissues and bone. CT scans use ionizing radiation, which can cause long term side effects such as cancers<sup>13, 14</sup>. It also is difficult to distinguish between different soft tissues and is most commonly used for structural imaging, such as bone and vascular systems<sup>6</sup>. MRI uses a pulsing strong magnetic field and relies on differences in the relaxation times of biological molecules to create an image of soft tissues<sup>15</sup>. The strong magnetic field can potentially interact with any implant or foreign metal in the body. It also can be quite uncomfortable for patients<sup>6, 15</sup>. Optical imaging uses light in the ultraviolet, visible, or near infrared regions of the spectrum and relies on differences in the spectral properties of biological species to compose an image<sup>7</sup>. This type of imaging is of great interest as it is nontoxic and can provide deeper tissue imaging with enhanced spacial resolution<sup>1, 2</sup>.

Often, to better differentiate between different biological species, contrast agents are used. Contrast agents highlight areas of interest providing better visualization<sup>3</sup>.

Ultrasound uses microbubbles, which are micron sized lipid or protein shells filled with gas which have a high echogenicity. This can be injected intravenously to monitor blood flow and perfusion in organs<sup>16</sup>. CT scans can use iodine or barium based markers,

depending on the area of interest, which can be administered orally, rectally, or intravenously<sup>3</sup>. Areas containing the agent have greater attenuation which provides “dark” areas on the resulting image<sup>13</sup>. MRI uses gadolinium contrast agents which are paramagnetic and react to strongly to the magnetic field providing intense signals<sup>17</sup>. Optical imaging uses fluorescent dyes which absorb and emit light to produce a stronger signal at areas of interest<sup>4</sup>. All of these techniques provide a better signal to background ratio.

In many cases, these contrast agents come with their own side effects which can be quite serious. Microbubbles used in ultrasound are fairly harmless, however if they rupture, they can rupture small vascular systems in the area<sup>10, 16, 18</sup>. Iodine based contrast agents used in CT scans are known to cause allergic reactions and renal problems including kidney failure and death<sup>14, 19, 20</sup>. Gadolinium, used in MRI, is a heavy metal which, when unbound, is toxic. These agents rely on strong chelation to maintain limited toxicity, however ions may leach out causing nephrogenic systemic fibrosis which can lead to renal failure and the hardening of the lungs and heart<sup>15,17</sup>. In optical imaging indocyanine green (ICG) has been the industry standard for more than 50 years with limited toxicity reported<sup>2</sup>. Although this dye has proved its worth to the optical imaging community, there is an interest for new designer dyes which provide nontoxic, targeted visualization of specific molecular species<sup>5</sup>.

## Motivation

Optical imaging is of particular interest because of its nontoxic nature<sup>7</sup>. Using light in the ultraviolet or visible range has stringent depth restrictions, with maximum penetration of up to a few millimeters due to strong scatter and absorption from biological species.

There is, however, an optical or therapeutic window in tissues where deeper penetration is possible. Between 600-1000 nanometers, penetration is increased due to a decrease in absorption and scatter from abundant species such as water and hemoglobin<sup>2,4,5</sup>. Using agents which absorb and emit in this region allows for increases up to several centimeters. If more photons are able to penetrate through to the target and then make it back to the detector without being scattered or reabsorbed then a stronger signal and better visualization is achieved and a lower concentration can be used to decrease risks of side effects, such as allergic reactions<sup>2,5</sup>.

Indocyanine green has been in use for more than 50 years. It has little reported toxicity and its absorption and emission are within the optimal range for minimized background absorbance<sup>21</sup>. Although it is useful for some applications, there is a desire for more exotic, specialized dyes which have tuned spectral properties and can be targeted to a specific molecular species<sup>5</sup>. Binding with a species known to accumulate at the site of interest provides an increase in contrast in the resulting image. Targeting can be achieved through the incorporation of moieties which are reactive with those present on the species of interest<sup>1,4,5</sup>.

## Research Goals and Approach

It was our goal to create a new fluorescent probe, which would absorb and emit within the optical window and provide targeted optical visualization of proteins which are often overexpressed at the surface of tumors. We first needed to investigate an appropriate dye which provided a strong signal within the optical window at low toxicities. Then we needed to incorporate a protein specific targeting moiety which would provide a means for biological conjugation. Finally we needed to synthesize and conjugate the probe to a model protein, bovine serum albumin (BSA) in this system, to ensure that binding can indeed occur<sup>5, 22</sup>.

When looking for a potential dye, it was noted that carbocyanine dyes have been widely investigated as contrast agents in NIR *in vivo* imaging<sup>1, 24</sup>. Cyanine derivatives are known to absorb and emit between 500-900nm depending on the length of the methanine bridge, the heterocyclic nuclei, as well as any species bound to the main scaffold<sup>23-25, 25</sup>. Increasing the length and conjugation of the bridge increases the absorption wavelength. However this also increases reactivity, subsequently lowering the stability<sup>26</sup>. Indocyanine green is a cyanine-7 (Cy7) derivative with 7 carbons in this methanine bridge<sup>23</sup>.

The particular cyanine derivative we are interested in is a cyanine-5 (Cy5) dye is known to absorb and emit at 642 and 658nm, which is within the optical window. It has also been shown to incorporate three different functionalities, two of which are commonly

used in click type reactions<sup>1</sup>. Azide and alkyne functionalities, in the presence of sodium ascorbate and copper (II) sulfate, readily take part in Huisgen cycloadditions<sup>27</sup>. This provides a simple means of attachment for a bio reactive moiety.

The objective was to link a carbocyanine Cy5 dye to a protein or antibody. N-hydroxysuccinimide (NHS), which is a common cross linker used in standard methods for dye attachment to protein was investigated and modified with an azidopropane derivative<sup>28</sup>. This azide functionality made it “click-able” to the alkyne containing dye<sup>29</sup>. With this lysine reactive moiety, the dye should be targeted toward proteins or antibodies. In this case, BSA was used as a model system to determine if the modified NHS would bind.

An appropriate dye with the desired properties was determined along with a means for the attachment of this dye to a biological molecule. This was accomplished through a pentamethine cyanine dye containing an alkyne moiety which has been attached to an NHS based linker through click chemistry methods, resulting in a stable 1, 2, 3 triazole. The final molecular probe was shown to maintain its spectral characteristics in preliminary results when bound to a protein, BSA.

## Thesis Outline

In this thesis, a literary review is presented as a justification for the pursuit of a fluorescent dye which is able to conjugate and act as a targeted probe. This highlights



medical imaging and contrast agents, desired spectral properties which go into the choice of a fluorescent dye, methods used for targeting, and an overview of the system of study. This is followed by an experimental section where procedure for the synthesis, assembly of the molecular probe, and bioconjugation will be discussed. The results and conclusions discuss the findings of the research which is followed by potential future work to advance the project.

## CHAPTER TWO

### LITERATURE REVIEW

#### Imaging

Biological imaging is widely used in both clinical and research fields to reveal, diagnose, and examine disease. It provides a means for early detection through noninvasive visualization of specific molecular targets<sup>8,30</sup>. The most commonly used types of imaging include ultrasound sonography, computed tomography (CT), magnetic resonance imaging (MRI), and optical imaging<sup>3,6</sup>. All rely on the detection of differences in the composition of biological features to create an image. This detection can be based on differences in echogenicity in the case of ultrasound, density as with CT scans, chemical composition as with MRI, or spectral properties in the case of optical imaging<sup>2,4,14,31</sup>,

Sonography, or ultrasound, is one of the safest forms of medical imaging<sup>6</sup>. Sound waves are introduced to the body and echoes are detected and used to create an image, much like a bat uses echolocation to gain awareness of its surroundings<sup>11</sup>. From a cost standpoint, it is one of the least expensive types of visualization available. However, ultrasound is severely limited by depth and the presence of bone and air in the system<sup>12</sup>. Areas surrounded by bone or filled with air cannot be clearly imaged using this technique, including the brain, chest cavity, gastrointestinal tract, and lungs<sup>10,11</sup>. With increasing obesity rates, penetration depth is becoming more of a concern, especially in pregnant women<sup>12</sup>. Penetration depth can be increased by lowering the frequency;

however this also lowers the resolution of the resulting image. At higher frequencies, higher resolutions can be obtained, however this is accompanied by increases in attenuation (or loss of signal) and scatter, restricting penetration<sup>31</sup>. .

Computed tomography (CT) compiles a series of x-rays taken on a single axis of rotation to produce an image in nearly real time. CT scans detect differences in density, making resolution between soft tissues low. It is best suited for imaging of structural aspects such as bone, bowel, and vascular systems<sup>6, 13</sup>. The major concern with CT scans is the dose of ionizing radiation the patient receives, which can be 30-400 times that of a single x-ray depending on the location and extent of visualization required. It is estimated that as of 2007 as many as 0.7% of cancers in the United States are caused by CT imaging. With an increase in use and overuse, this number is expected to increase up to 2%<sup>14, 32</sup>. Half of the ionizing radiation an American sees in his or her lifetime is due to medical imaging<sup>14</sup>. Another downfall with CT scan is patient movement which can blur the resulting image, requiring another scan<sup>6, 32</sup>.

Magnetic resonance imaging (MRI) provides high resolution images in nearly real time with the use of a strong magnetic field. Although it does not use ionizing radiation, this field can interact with implants, such as pacemakers, and foreign metal lodged in the body<sup>15</sup>. This strong magnetic field is turned on and off in quick succession, measuring the relaxation times of different molecular species present. The pulsing field can also cause peripheral nerve stimulation, where extremities may twitch or move<sup>33</sup>. Like CT scans,

MRI images are also blurred by patient movement. MRI can be quite uncomfortable for some patients. Although open systems do exist, most are narrow cylinders which use a backboard to slide the patient inside, and often require restraining the head. This confined space accompanied by restraint and very loud noises can be intolerable for even mildly claustrophobic patients<sup>34</sup>. This is also limiting for obese patients who may be too wide or over the weight limit of the table<sup>6,35</sup>.

Optical imaging uses light in the ultraviolet (UV), visible, or near infrared (NIR) regions to distinguish between molecular species based on their spectral properties<sup>2</sup>. This type of imaging is of great interest due to its nontoxic nature and its ability to produce visualization with high spacial resolution between soft tissues. Light which enters the body is absorbed and scattered by abundant species such as water, blood, and skin<sup>7</sup>. There exists an optical window between 600-1000nm where maximum penetration is observed, this is seen in figure 1. At wavelengths outside this region, scatter and absorption restricts penetration to only a few millimeters. Light within the optical window can penetrate several centimeters. This technology can also be adapted to be used with an endoscope for even deeper tissue imaging<sup>2,7</sup>.

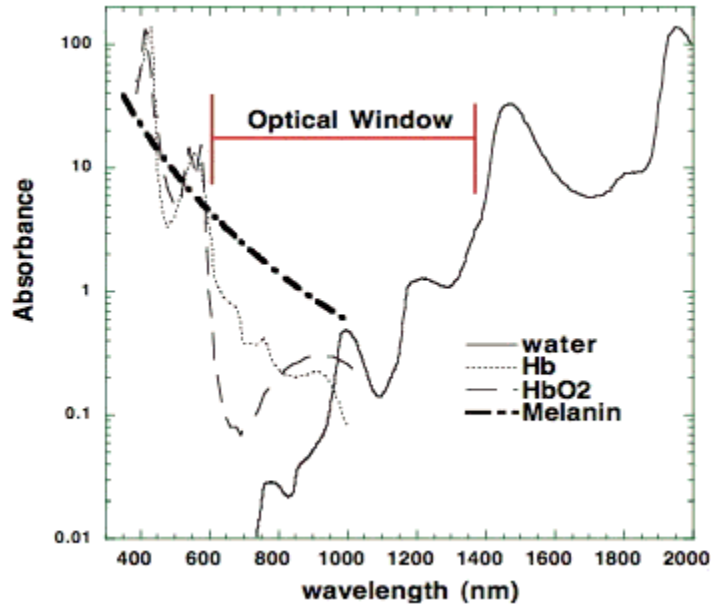


Figure 1: The optical window is clear by looking at the absorbance spectra for prevalent biomolecules: water, hemoglobin (Hb), oxygenated hemoglobin (HbO<sub>2</sub>), and melanin<sup>36</sup>.

### Contrast Agents

Often to better distinguish between the background and the region of interest different contrast agents are used. Contrast agents are available for all major imaging techniques and can provide better visualization of areas of interest<sup>3</sup>. Some contrast agents are harmless, like microbubbles in ultrasound and the use of indocyanine green in optical imaging. Microbubbles are simply micron sized bubbles of gas surrounded by a lipid or protein shell which have a high echogenicity. When injected, they provide areas of high signal which can be used to investigate blood flow, lesions, and perfusion in organs<sup>16, 37, 38</sup>. This can be seen in figure 2, showing a renal carcinoma as seen with and without the use of microbubbles during imaging<sup>37</sup>. With contrast agent, the signal to noise ratio is

clearly increased. Indocyanine green (ICG) is a cyanine based fluorescent dye used in optical imaging. It has been the industry standard fluorescent dye for more than 50 years with little toxicity reported<sup>21</sup>. In figure 5 a rat has been imaged using ICG to map different organs based on its progress through the body<sup>39</sup>.

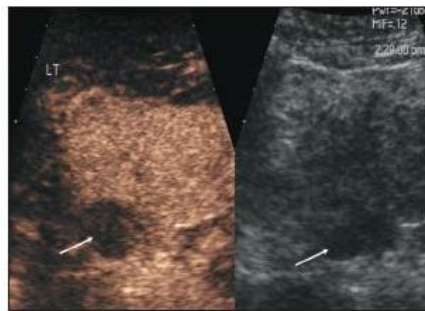


FIGURE 3. Renal cell carcinoma. Note low reflective area showing some abnormal enhancement (arrow).

Figure 2: Ultrasound image of a renal carcinoma (denoted with white arrow), with (left) and without (right) the use of microbubbles as a contrast agent<sup>38</sup>.

Some contrast agents are not as benign. CT scans with and without the use of contrast agent can be seen in figure 3, the difference in visualization ability is undeniable<sup>40</sup>. However, iodine based agents can cause severe allergic reactions as well as contrast induce neuropathy<sup>19</sup>. This can cause kidney damage and failure. Although rare, it is a problem for a high risk population consisting of individuals with diabetes and the elderly, both growing in the United States<sup>20</sup>. Figure 4 shows a cranial MRI with and without imaging agent, an arrow is used to indicate the site of a lesion<sup>41</sup>. Although helpful, MRI

gadolinium contrast agents also cause kidney problems. This type of agent relies on strong chelation of the gadolinium ion, which when unbound is highly toxic<sup>17</sup>.

Nephrogenic systemic fibrosis is a disease attributed to the leaching of these ions. This disease causes hardening of the skin, which can spread to the heart and lungs causing failure and death<sup>15, 17</sup>. It can also cause kidney failure and minor side effects such as headache and nausea. The elderly and the diabetic population are again at a greater risk for the more serious side effects. Although serious problems are rare, they are not unheard of and with the increase in use are likely to become more common<sup>17, 34</sup>.

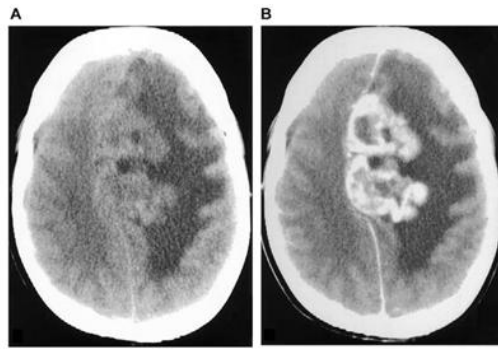


Figure 3: A CT scan of the brain without (left) and with (right) contrast agent<sup>40</sup>.

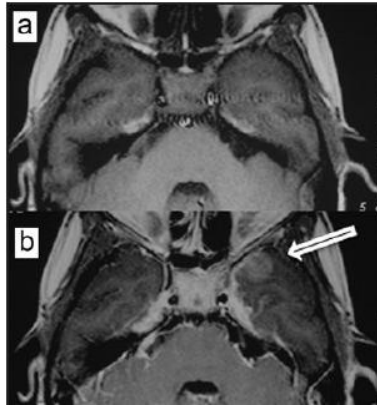


Figure 4: A MRI image of a nodule in the temporal lobe, as seen with (bottom) denoted with a white arrow, and without (top) contrast agent<sup>41</sup>.

### Targeting

Optical imaging is of great interest due to its ability to obtain high resolution visualization of deep tissues. The combination of resolution with safety makes it a more viable source of visualization for a wide range of uses. Figure 5 shows a composite of 9 optical images, mapping internal organs based on the rate indocyanine green (ICG) passes through the body<sup>39</sup>. Fluorescent dyes provide even higher visual contrast, which enables better differentiation of different species present<sup>4,5</sup>. Although ICG has been used for over 50 years, there is an interest in new specialized dyes which can be targeted to label specific molecular species. Targeting facilitates the accumulation of dye at a particular site of interest, which can allow for better imaging at a reduced concentration, in turn reducing toxicity risks<sup>2,4,30</sup>.



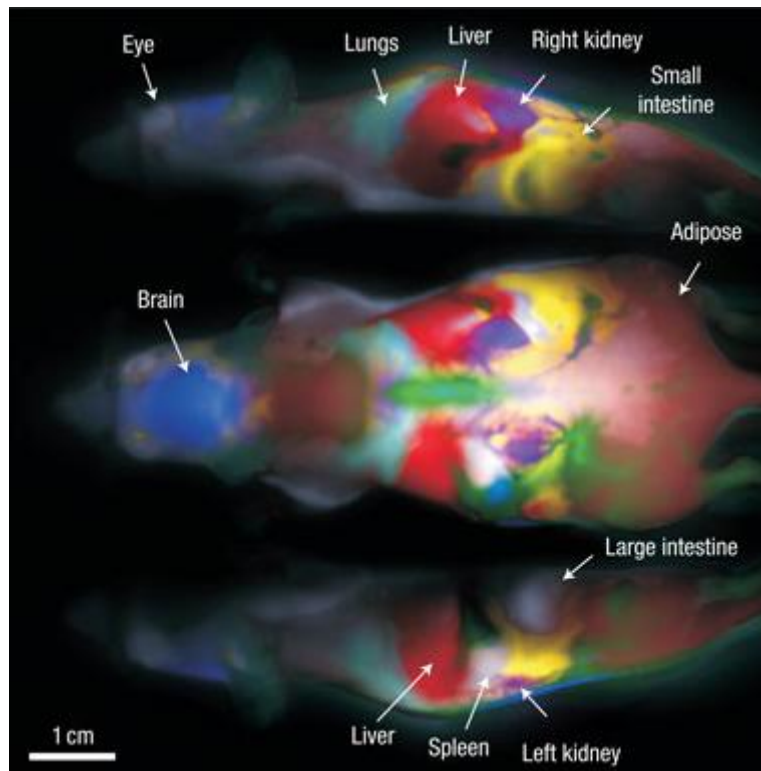


Figure 5: Composite of 9 optical images of a rat using ICG to map different internal organs non-invasively<sup>39</sup>.

By targeting biological molecules which are influenced by the presence of disease, such as the response of an antibody or protein at the site of abnormality, a more distinct picture of the infected area can be established. This can be very helpful when monitoring treatment. Targeting is the binding of a probe or marker with a biological species or synthetic polymer. Small molecules are often used in an attempt to suppress potential immune responses<sup>2, 4, 42, 43</sup>. In this model system, we will focus on the targeting of lysine containing species such as proteins<sup>28</sup>.

Proteins are commonly labeled using n-hydroxysuccinimide (NHS) derivatives as cross linkers. Derivatives containing the NHS moiety are very reactive with primary amides found in lysine. This allows for the specific labeling of species which contain accessible lysine binding sites<sup>28</sup>. Tumors often overexpress proteins on their surface, targeting of such proteins can provide an accumulation of contrast agent at the site providing a clear outline of disease<sup>4, 44</sup>.

### Design of Molecular Probe

There are many aspects which need to be considered in the design of a new molecular probe. For optical imaging, spectral characteristics are extremely important. For the probe to be optically active it must contain a chromophore. To be targeted it must contain a bioactive moiety or the means for attachment, such as a functional group. It should be both photo and chemically stable, have strong spectral characteristics to provide a high signal to noise ratio, and have desired pharmacological attributes such as a low toxicity and aqueous solubility<sup>5, 45</sup>.

Probes must react with specific biological molecules<sup>43</sup>. Usually binding is limited to one dye per binding site with potential for a number of sites<sup>46</sup>. They should be selective, designed with moieties able to conjugate with only the species of interest<sup>47</sup>. Ideally these probes should be nontoxic with no mutagenic or carcinogenic effects and be eliminated from the body in a reasonable timeframe. They should also strongly absorb and emit at

different wavelengths within the optical window<sup>48</sup>. All characteristics must be addressed for a probe to be a feasible candidate for *in vivo* optical imaging<sup>49</sup>.

### Spectral Properties

A species spectral characteristics describe the way it interacts with light. This becomes extremely important for any dye considered in optical imaging. The most important characteristics are the absorbance and emission wavelengths, the molar absorptivity, the Stokes shift, and the quantum yield. The absorbance intensity is the extent light energy is taken in or absorbed by a particular species; the emission is the release of that energy in the form of light at the same or at a different wavelength. Different chromophores absorb and emit at different wavelengths depending on the energy spacing between the highest occupied molecular orbital (HOMO) and lowest unoccupied molecular orbital (LUMO). The difference between the absorption and emission wavelengths is the Stokes shift<sup>50</sup>. A large Stokes shift is desirable for several reasons. If a dye exhibits a large Stokes shift then you can excite the sample at one wavelength and use filters and a detector to capture the emission at a different wavelength. A large shift limits the probability of reabsorption which weakens the signal<sup>2</sup>.

The molar absorptivity is the absorbance intensity per unit molar volume. It can be thought of as a measure of the brightness of the dye. High molar absorptivity allows for strong signals at lower concentrations, which decreases problems associated with toxicity

as well as aggregation. The quantum yield (QY) is an important factor in achieving a high signal to noise ratio<sup>50</sup>.

Quantum yield is a measure of the fluorescence efficiency. It can be thought of as the ratio of the number of absorbed to emitted photons. The higher the quantum yield the higher the percentage of absorbed photon energy is released as light, allowing for stronger signals at lower concentrations. Quantum yield can be reported in two ways: the absolute quantum yield, which requires very precise information about the exact number of photons received by the samples, and the relative method which calculates the quantum yield of an unknown based on that of a well characterized standard. Reporting the exact method of determination is critical as the quantum yield can change considerably with the surround environment, bound or unbound. It may drastically shift with each structural change as well as with differences in solvent, and therefore should be calculated for all intended environments. We will be determining quantum yield based on the relative method using water as a solvent. The relative method is preferred in this case as it accounts for solvent differences between the unknown and the standard by incorporation of the ratio of refractive indexes. Differences in reported relative quantum yield are common, distortions in measurements can occur with errors in the absorbance intensity and if fluorescence varies nonlinearly with concentration. Absorbance intensities should be no higher than 0.05 to minimize this error<sup>51</sup>. Other sources of error include filter effects, bad dissolution or variations in concentration, the presence of

gaseous oxygen present in the sample, impurities, and instabilities all of which can cause false intensities at either higher or lower than true values<sup>51, 52</sup>.

The absorption and emission wavelength are extremely important for biological fluorescent dyes because there is such high scatter and absorption from prevalent species such as water, hemoglobin, and melanin<sup>53</sup>. Scatter cause by biological species is Rayleigh type scattering which is proportional to the inverse of the wavelength to the fourth power. This means that at longer wavelengths there is less scatter allowing for a lower background signal<sup>54</sup>.

Although longer wavelengths give less scatter, beyond 1000nm problems with absorption are seen. There is an optical window when absorption is minimized and signal to background ratios can be optimized between 600-1000nm. Outside this range, problems with scatter and/or absorbance limit penetration up to a few millimeters at best. Within this range, however, depths up to several centimeters can be realized. Also, because optical imaging technology can be adapted to fit endoscopic means, even deeper penetration depths can be obtained. This can help ease imaging problems for the obese population<sup>2, 5, 7</sup>.

## Cyanine

Cyanine dyes, such as ICG, have been investigated for their use in various applications of optical imaging. Cyanines are known to absorb and emit at longer wavelengths in part to

a structural aspect known as the methanine bridge. This conjugated bridging section can produce a red shift of 80-100nm to the absorption wavelength of the chromophore with each double bonded carbon<sup>46</sup>. Cyanine dyes are categorized by the number of carbons in this bridging section. Cyanine 3, 5, and 7 (Cy3, Cy5, and Cy7) have increasing absorbance and emission wavelengths<sup>23</sup>. Cy3 dyes typically absorb around 500-600nm (seen in figure 6), Cy5 dyes absorb around 600-700 (seen in figure 7), and Cy7 dyes absorb around 700-800 (seen in figure 8). This broad nomenclature applies regardless of heterocyclic nuclei and moieties present which also influence the resulting wavelength. Although Cy7 dyes absorb further into the optical window, this comes with an increase in the reactivity of this methanine bridge<sup>55, 56</sup>. Increases in reactivity cause a decrease in stability which may be both photo and chemical in nature. Several carbocyanine derivatives have been applied in bioconjugation and targeting of species and show high biocompatibility. Commercial cyanines are available for the labeling of biological species such as DNA<sup>15,55,57,1, 58</sup>.

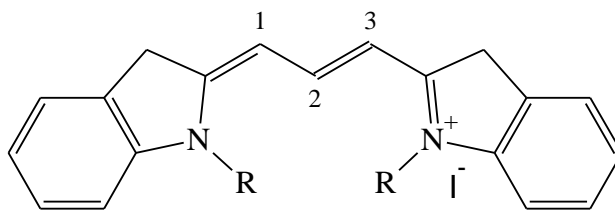


Figure 6: Cyanine 3, or Cy3, derivatives contain three carbons in the methanine bridge and usually absorb and emits between 500-600nm.

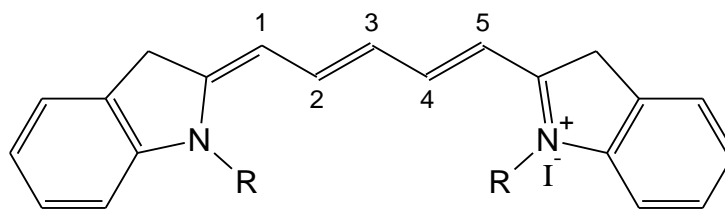


Figure 7: Cyanine 5, or Cy5, derivatives contain five carbons in the methine bridge and usually absorb between 600-700nm.

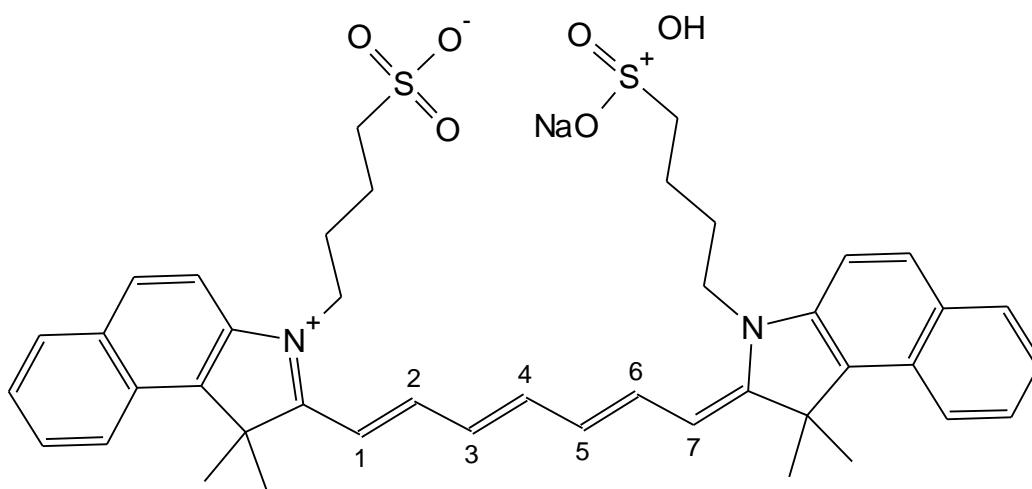


Figure 8: Indocyanine Green (ICG), a Cy7 type dye which has been used in the optical imaging field for over 50 years.

### Cross linkers

Cross linkers are a group of species known to provide a source of binding between two otherwise unbindable species. We are particularly interested in n-hydroxysuccinimide (NHS) a commonly used cross linker which reacts readily with primary amides. The structure of NHS can be seen in figure 9. Lysine, an amino acid, is known to contain these primary amides. Incorporation of an NHS moiety is a common method which

allows a dye to label proteins. This is generally done with the ester variety, but in this case NHS was modified to contain an azidopropane derivative without the ester functionality<sup>28, 29</sup>.

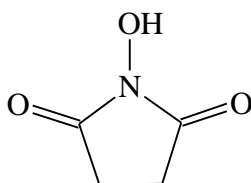


Figure 9: N-hydroxysuccinimide (NHS) is a cross linker which is commonly used in the labeling of proteins or species containing primary amides.

### Proposed Design

The dye we are interested in is an asymmetric carbocyanine dye introduced by Shao, et al.,<sup>1</sup>. This dye presents several advantages such as a strong absorption and emission within the optical window, a reasonable quantum yield, and a low toxicity seen in previous testing *in vivo*. This dye has also been shown to incorporate three different functional groups, two of which are known to participate in click type reactions<sup>1</sup>.

Alkyne and azide functionalities in the presences of copper (II) sulfate and sodium ascorbate are known to participate in a Huisgen cycloaddition resulting in the formation of a stable 1, 2, 3-triazole. Click reactions are known for their high product specific yields using benign solvents at low temperatures. They are often utilized for the



synthesis of large, complicated structures through the assembly of smaller modular units. Because of the high thermodynamic driving force, these reactions proceed quickly and predictably<sup>27, 59</sup>. By incorporating this functionality in the final dye, a means for attachment to a linker could be realized. An azidopropane NHS species which is targeted to a specific molecular species was chosen to facilitate the targeting of the cyanine dye of interest. When assembled, this dye-linker pair will act as a molecular probe, targeted towards proteins. In this model system, the protein is BSA, if it can be determined that binding does indeed occur, the work can be applied to specific proteins known to be overexpressed during tumor growth. The final proposed probe can be seen in figure 8.

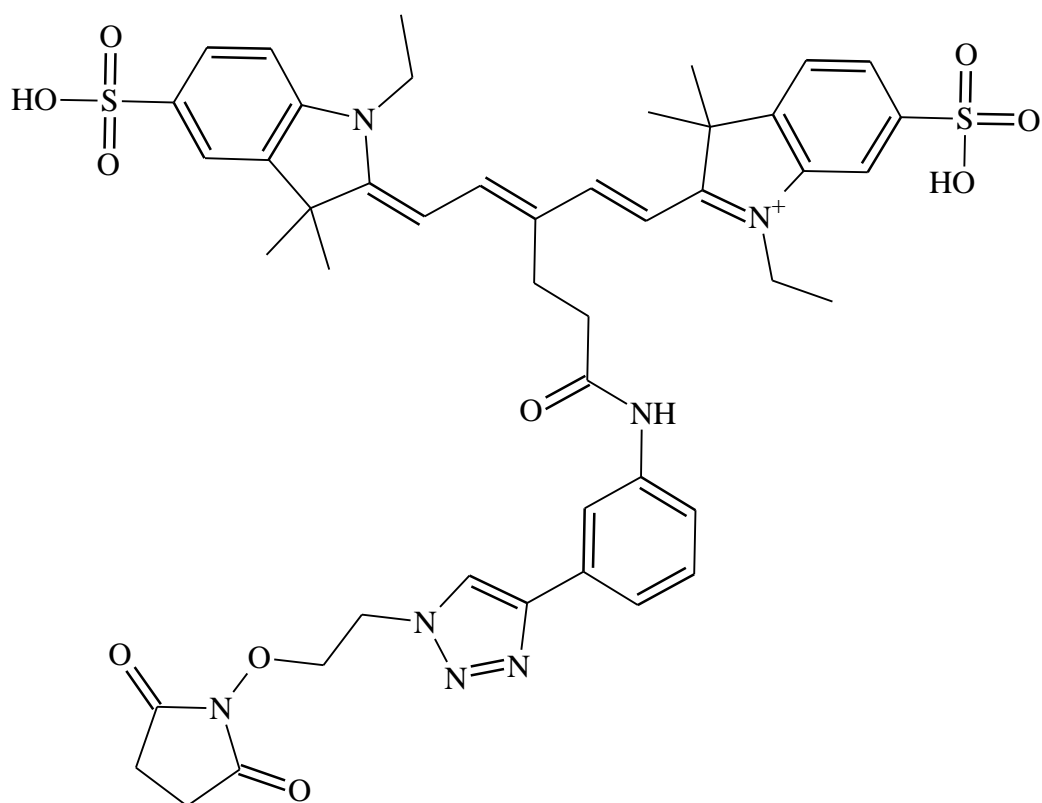


Figure 10: Chemical structure of synthesized molecular probe consisting of pentamethine carbocyanine backbone

## CHAPTER THREE

### EXPERIMENTAL

#### Instrumentation and Reagent Information

Dimethyl formaldehyde (DMF), pyridine, tetrahydrofuran (THF), acetic acid, isopropanol, chloroform, dichloromethane (DCM), dimethylsulfoxide (DMSO) was received from Acros. Potassium hydroxide, copper (II) sulfate, and sodium ascorbate were obtained from Aldrich. 3-methyl-2butanone and iodoethane were obtained from Alfa Aesar. Bovine serum albumin (BSA) was obtained from Baker. Micro dialysis float units, hydrochloric acid, and sodium sulfate were obtained by Fisher Scientific, Potassium carbonate was obtained from Fluka, phosphate buffer solution (PBS) was obtained from Thermo Scientific, N-hydroxysuccinimide was obtained from TCI, and methanol, diethyl ether and acetone were obtained from VWR. Methyl 5, 5 dimethoxyvalerate, hydrazine benzene, and (Azidopropane) were prepared previously by Yurii Bandera.

Tetrahydrofurane (THF) was purified with an IT PureSolv solvent purification system. Rotary evaporation was done using a Büchi rotovapor R-200. All masses were recorded using an Ohaus Explorer analytical balance. Centrifuge was done using a Beckman J2-21 high speed refrigerated centrifuge. All  $^1\text{H}$  and  $^{13}\text{C}$  NMR were taken on a Joel ECX-300 relative to tetramethylsilane (TMS), the internal standard. All absorbance was done on a Perkin Elmer Lambda 850 spectrometer. Fluorescence intensities were recorded using a

Horiba Jobin-Yvon microHR spectrometer coupled to a synapse charge coupled device (CCD).

### Preparation of Dye

All dye synthesis was according to Shao, et al., and was carried out with minor changes in the initial preparation of the dianil intermediate<sup>1</sup>. A final reaction scheme between two synthesized intermediates is seen in figure 10.

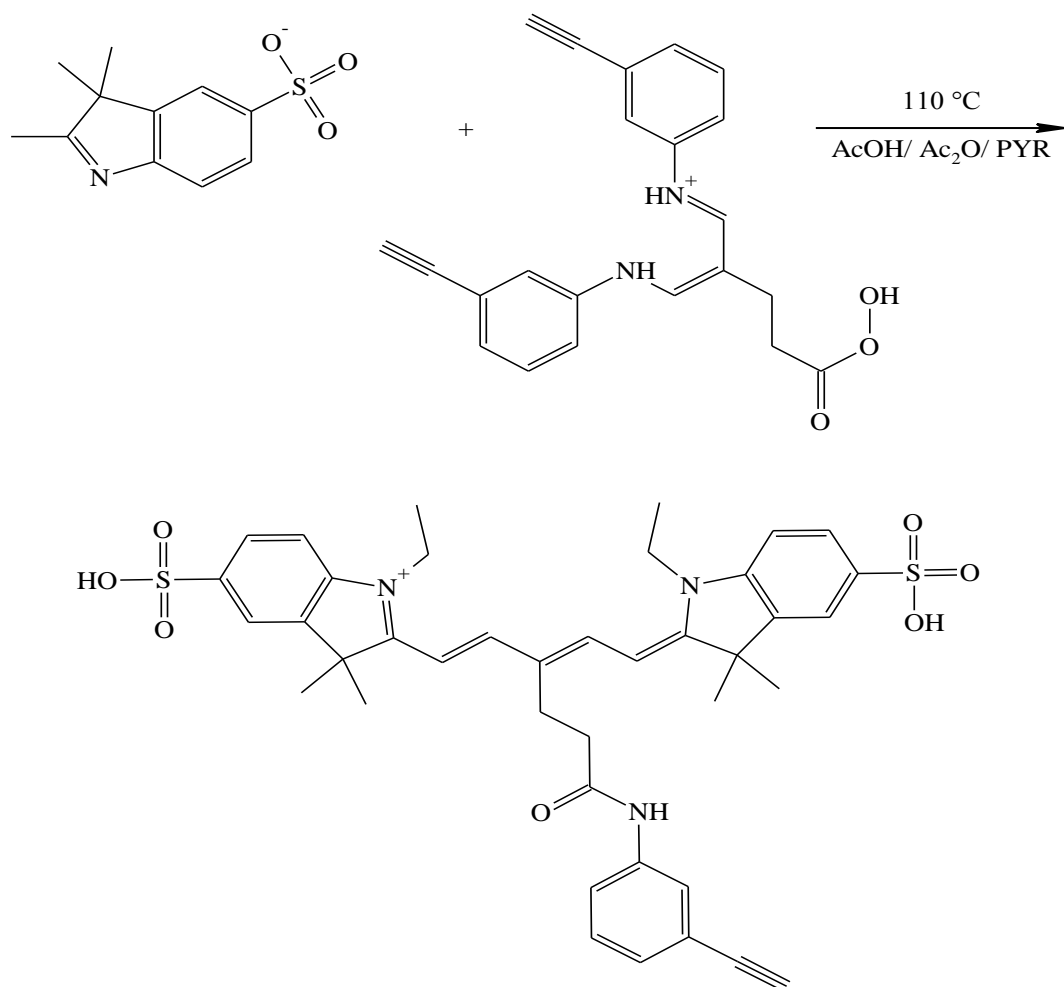


Figure 11: Final dye synthetic route

*Synthesis and Hydrolysis of 5-(Phenlamino)-4-(phenylimino) methyl)-  
4-pentenoic Acid Derivative*

The general scheme for the first intermediate can be seen in figure 12.

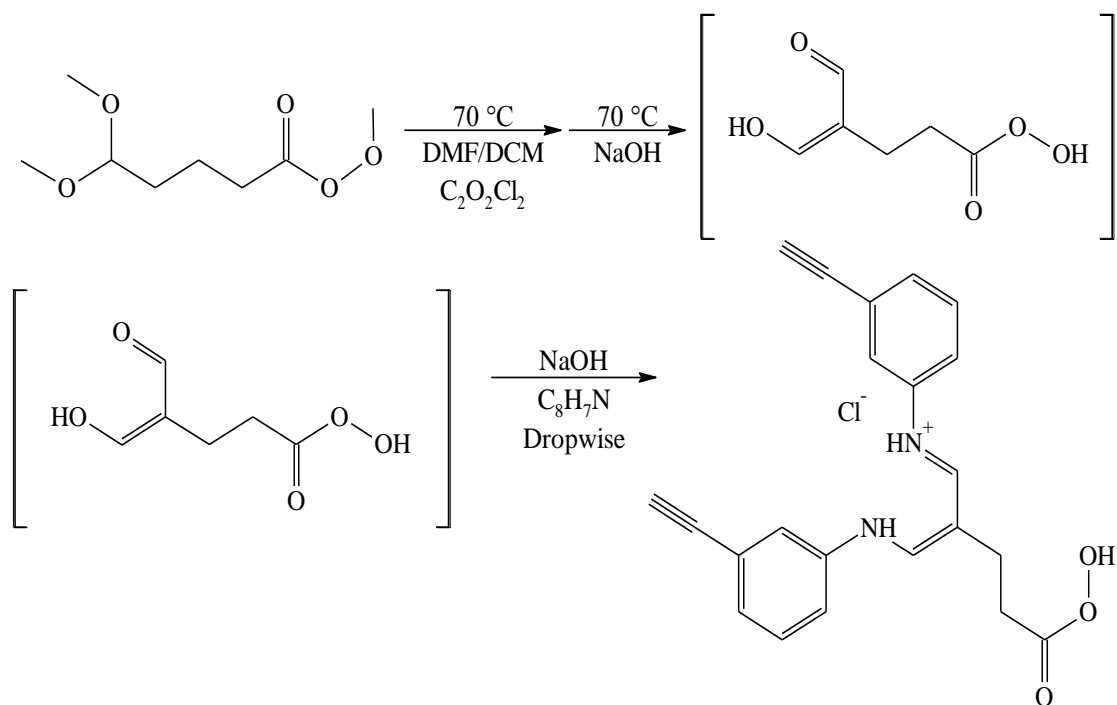


Figure 12: Synthetic route for the alkyne intermediate.

A 1:3:1.5:3 molar ratio of methyl 5,5 dimethoxyvalerate, dimethyl formaldehyde (DMF), phosphoryl chloride, and 3-ethynylaniline was used, which was a deviation from the procedure found in Shao, et al.,<sup>1</sup>. DMF and phosphoryl chloride were combined with stirring and a heat gun was used to raise the temperature to  $70\text{ }^\circ\text{C}$ , turning the solution from colorless to red. After cooling, methyl 5,5 dimethoxyvalerate was added drop wise and the reaction was stirred for 6 hours at room temperature. 3-ethynylaniline, which provided the alkyne functionality, was dissolved in methanol and added to the reaction flask, which was then stirred at room temperature overnight. A crude yellow product was precipitated in water and dried. This ester intermediate was then dissolved in THF before

the addition of an aqueous sodium chloride solution. This was then acidified with hydrochloric acid and a crude product was precipitated in excess THF. The solvent was removed via rotary evaporation resulting in a yellow product which was filtered and used without further purification.

Product was verified by  $^1\text{H}$  NMR (301 MHz,  $\text{DMSO-}d_6$ )  $\delta$  ppm 8.92 (s, 2H), 7.41 (s, 1H), 7.37 (d, 2H,  $J=7.2\text{Hz}$ ), 7.34 (d, 2H,  $J=8.0\text{Hz}$ ), 7.2 (d, 2H,  $J=6.8\text{Hz}$ ), 4.24 (s, 2H), 2.79 (t, 2H,  $J=7.5\text{Hz}$ ), 2.44 (t, 2H,  $J=7.8\text{Hz}$ ). Yield was comparable to literature at about 23%.

#### *Preparation of potassium 2, 3, 3-trimethyl-3H-indole-5-sulfonate*

A reaction scheme for this indolinium salt intermediate is shown in figure 13.

A 1:2 molar ratio of hydrazinobenzene sulfonic acid and 3-methyl-2-butanone were dissolved in a 4:1 volumetric ratio of acetic acid and acetic anhydride. The solution was refluxed between 3-5 hours, sometimes overnight before the solvent was removed via rotary evaporation. The resulting residue was dissolved in methanol and a saturated solution of potassium hydroxide in isopropanol was added. This was allowed to reflux for 10 minutes before it was cooled to room temperature. After cooling crude product was precipitated in excess diethyl ether, filtered, and dried. A 1:3 molar ratio of this potassium intermediate and iodoethane were combined in acetonitrile and refluxed

overnight. After cooling, the resulting violet solid was filtered and washed with acetone before being dried.

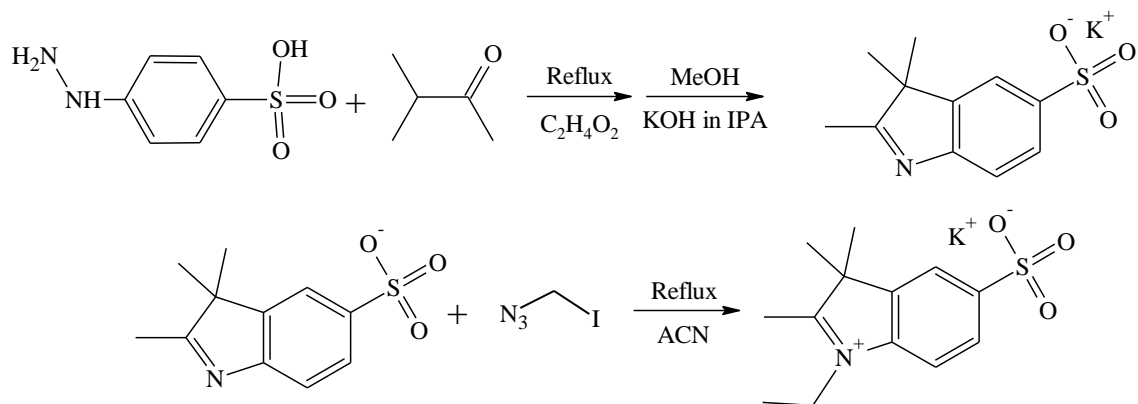


Figure 13: Synthetic route for the preparation of the indolinium salt intermediate, a reagent in the final dye

The product was verified by  $^1\text{H}$  NMR (301 MHz,  $\text{DMSO-}d_6$ )  $\delta$  ppm: 7.63 (d, 1H,  $J=1.5\text{Hz}$ , H-4), 7.56 (dd, 1H,  $J=7.9, 1.5\text{Hz}$ , H-6), 7.34 (d, 1H,  $J=7.9\text{Hz}$ , H-7), 2.21 (s, 3H), 1.24 (s, 6H). Yield 58%.

#### *Preparation of final dye*

The dianil intermediate was dissolved in a 15:5:1 volumetric ratio of acetic anhydride, acetic acid, and pyridine, which was heated to  $100^\circ\text{C}$ , and stirred for 2 hours before the



addition of the indolinium salt intermediate. This reaction was brought back up to temperature and stirred for an additional hour. The resulting solution was cooled and added drop wise to excess diethyl ether to precipitate a crude product. The precipitate was separated by centrifuge then purified using silica gel column chromatography with a 1:3 ratio of methanol to chloroform. This resulted in 85 grams of dark blue product, about 70% yield.

Verification was done via  $^1\text{H}$  NMR (301 MHz,  $\text{DMSO}-d_6$ )  $\delta$  ppm 10.08 (s, 1H), 8.19 (d, 2H,  $J=14.2\text{Hz}$ ), 7.82 (s, 2H), 7.79 (s, 1H), 7.64 (d, 2H,  $J=8.4\text{Hz}$ ), 7.48 (d, 1H,  $J=8.8\text{Hz}$ ), 7.33 (d, 2H,  $J=8.4\text{Hz}$ ), 7.25 (t, 1H,  $J=7.9\text{Hz}$ ), 7.07 (d, 1H,  $J=7.6\text{Hz}$ ), 6.38 (d, 2H,  $J=14.2\text{Hz}$ ), 4.21-4.18 (m, 4H), 4.05 (s, 1H), 2.98 (t, 2H,  $J=6.8$ ), 2.54 (t, 2H,  $J=6.8\text{Hz}$ ), 1.68 (s, 12H), 1.14 (t, 6H,  $J=7.3\text{Hz}$ ). The absorption and emission of the free dye were investigated in water. This can be seen in figure 14.

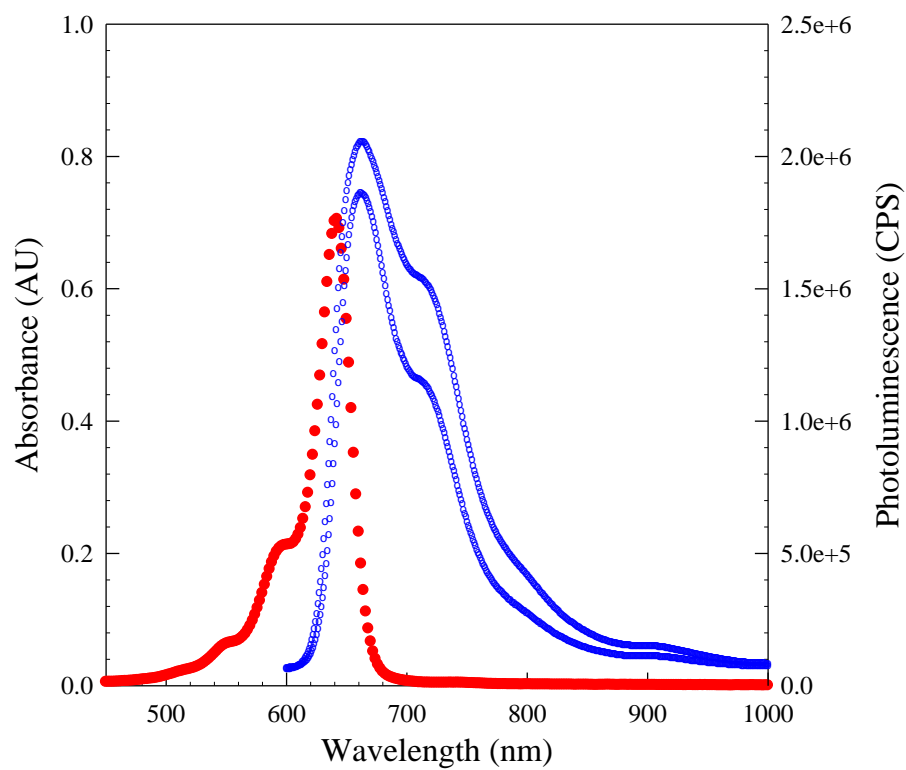


Figure 14: The absorbance (•) and emission (○) at 642nm excitation of the unbound dye in water.

#### Preparation of Linker

##### *Preparation of 1-(3-azidopropoxy) pyrrolidine-2, 5-dione*

A general scheme for the synthesis of the NHS derivative is shown in figure 15.

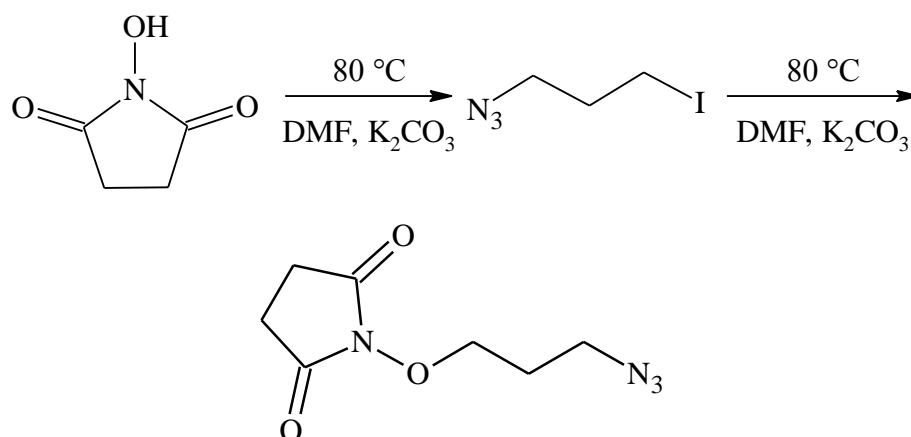


Figure 15: Synthesis of the cross linker (1-(3-azidopropyl) pyrrolidine-2, 5-dione)

A 1:1 molar ratio of 1-azido-3-iodopropane and NHS was used. Using potassium carbonate as a buffer, azidopropane was added to DMF at 80°C. This solution was allowed to stir for 10 minutes before the addition of NHS. After this addition the reaction was left at 80°C with stirring for 4 hours. After cooling, a crude product was precipitated by drop wise addition to diethyl ether. This product was then washed with deionized water and acidified with hydrochloric acid. The water layer was collected and the product was extracted with dichloromethane (DCM), which was then dried using sodium sulfate. After filtering, the DCM was removed via rotary evaporation. Remaining solvent was removed by the application of an air stream overnight. The final product was verified by  $^1\text{H}$  NMR (301 MHz,  $\text{DMSO-}d_6$ )  $\delta$  ppm 1.81 (t,  $J=6.47$  Hz, 2 H) 2.57 (s, 4 H) 3.49 (t,  $J=6.74$  Hz, 1 H) 4.02 (t,  $J=6.19$  Hz, 2 H). Yield 53%

This compound was thought to be unstable in water due to the reactivity of the NHS moiety. This was testing by immersing the oil in an aqueous environment for 1 week before extraction again with DCM, drying with sodium sulfate, filtering, and removing solvent. The remaining oil was verified by  $^1\text{H}$  NMR and showed no sign of degradation.

### Click Reaction

A copper catalyzed click type reaction was carried out in methanol, joining the azide functionality of the NHS derivative with the alkyne functionality of the dye. The general scheme of this Huisgen 1, 3 dipolar cycloaddition can be seen in figure 16 and the final proposed probe can be seen in Figure 8.

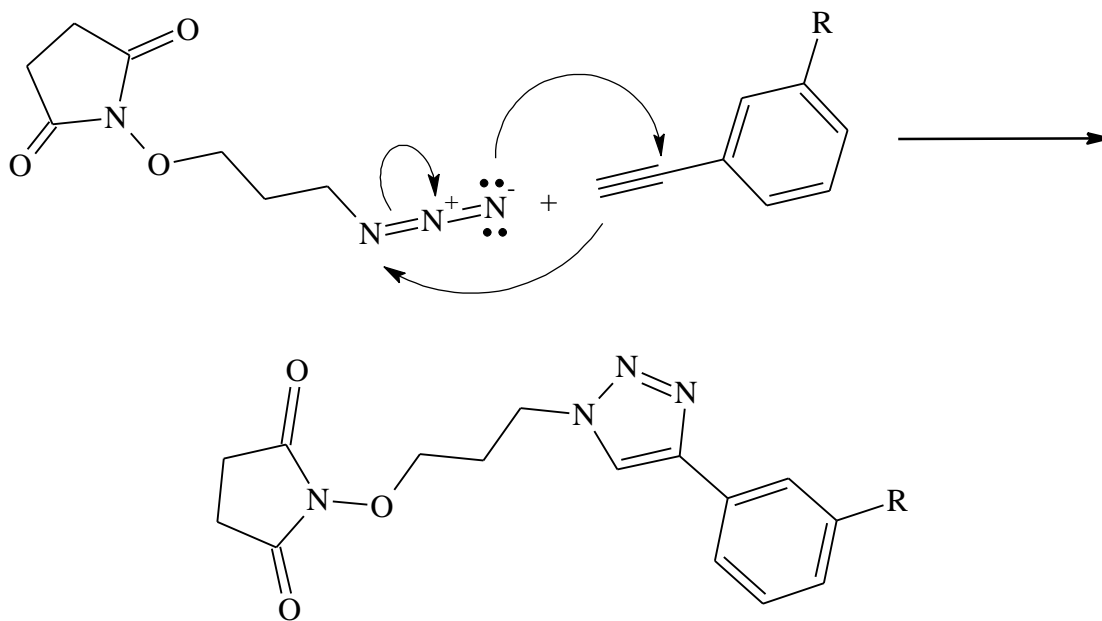


Figure 16: The Huisgen cycloaddition between an alkyne and azide.

1:1:2:10 molar ratio of dye, NHS derivative, copper (II) sulfate, and sodium ascorbate was used and the reaction was carried out in methanol. The dye, NHS derivative, and sodium ascorbate were combined in methanol with stirring at room temperature. After a 10 minute nitrogen purge, copper (II) sulfate was added and the reaction flask was sealed and allowed to stir for 2 days. After this time, a small sample was collected and run on a TLC plate in a 3:1 ratio of DCM to methanol. This ratio was used to separate products in silica gel column. The remaining product was cleared from the column using water. Two solutions were collected. The second dark blue product was verified to contain the 1, 2, 3 triazole by  $^1\text{H}$  NMR. (301 MHz,  $\text{DMSO-}d_6$ )  $\delta$  ppm 10.08 (s, 1H), 8.19 (d, 2H,  $J=14.2\text{Hz}$ ), 7.83 (s, 1 H) 7.82 (s, 2H), 7.79 (s, 1H), 7.64 (d, 2H,  $J=8.4\text{Hz}$ ), 7.48 (d, 1H,  $J=8.8\text{Hz}$ ), 7.33 (d, 2H,  $J=8.4\text{Hz}$ ), 7.25 (t, 1H,  $J=7.9\text{Hz}$ ), 7.07 (d, 1H,  $J=7.6\text{Hz}$ ), 6.38 (d, 2H,  $J=14.2\text{Hz}$ ), 4.83-4.81 (m, 4H), 2.98 (t, 2H,  $J=6.8$ ), 2.54 (t, 2H,  $J=6.8\text{Hz}$ ), 1.68 (s, 12H), 1.14 (t, 6H,  $J=7.3\text{Hz}$ ).

### Bioconjugation

Conjugation was carried out using a procedure outlined by Thermo Fisher Scientific<sup>28</sup>. A 14:1 molar ratio of probe to BSA was used. The molecular probe was dissolved in DMSO (1mg/100 $\mu\text{L}$  DMSO) before its addition to BSA in phosphate buffer (10mg/mL) solution (PBS). This solution was stirred at room temperature for 1 hour. The product was then purified by dialysis against PBS under refrigeration for three days, changing the

solution twice daily. It was determined the dialysis was complete when the final product no longer showed a loss in color. The absorption and emission were tested in PBS, the spectra is shown in figure 17.

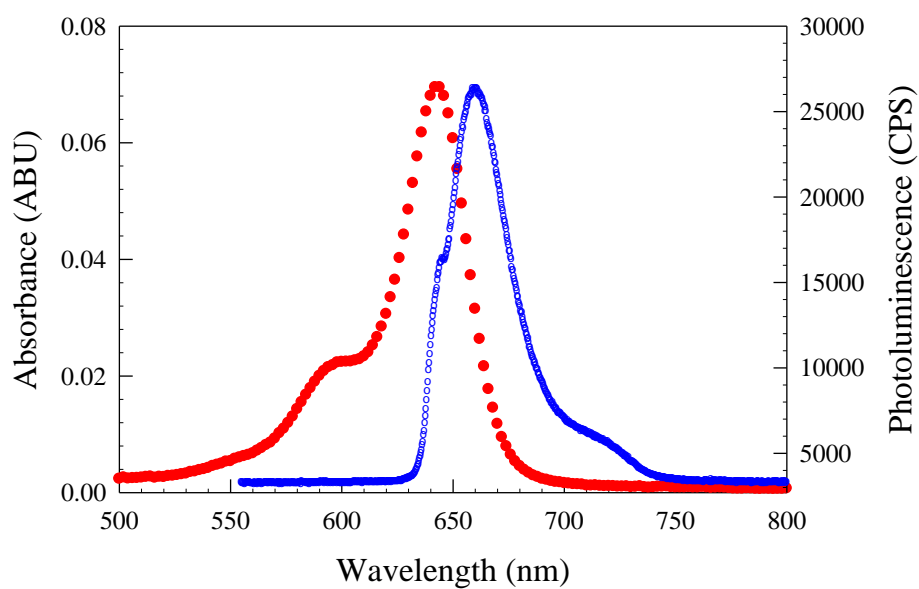


Figure 17: The absorbance (•) and emission (○) at 642nm excitation in PBS of the molecular probe when bound to BSA.

## CHAPTER FOUR

### RESULTS AND DISCUSSION

#### Synthesized Dye

In the preparation of the Cy5 dye, there were few modifications from the original procedure presented by Shao, et al., mainly the preparation of the initial intermediate as noted<sup>1</sup>.

This particular cyanine dye was comprised of a Cy5 scaffold with two identical monosulfonated indolinium moieties which provide excellent solubility in both methanol and water. This dye was chosen for its respectable reported yield of around 65%, which matches the yield for our slightly modified synthesis<sup>1</sup>. The desired alkyne functionality was introduced to the structure by the malonaldehyde dianil moiety. Verification of the final dye species was done through spectral and structural characteristics. NMR results show matching shifts for all major features and the absorption and emission were shown to be identical to literature, with maxima of 641 and 658nm respectively. This is a moderate Stokes shift of about 16nm. This shift is somewhat small for the probes intended purpose, but improvement may be an avenue of future study.

The dye showed strong absorption in aqueous solutions at micro molar concentrations. The molar absorptivity, found by Beer's law, equation 2, was around 144,000 L·M<sup>-1</sup>·cm<sup>-1</sup> in water, which was lower than the reported value which was 240,000 M<sup>-1</sup>·cm<sup>-1</sup> in PBS.

This difference may be attributed to error in concentration due to impurities or changes in pH between deionized water and PBS<sup>50</sup>.

$$A = \epsilon bc$$

Equation 1: Beer's law relates the absorbance intensity (A) with the molar absorptivity ( $\epsilon$ ), path length (b=1 cm), and concentration (c).

The quantum yield ( $\Phi$ ) was found to be 0.20 (or 20%) in water relative to zinc phthalocyanine (ZnPc) in DMF ( $\Phi=18\%$ ), matching literature. In order to calculate the relative quantum yield, the absorbance and emission at 642nm data for a known standard, ZnPc, and the unknown sample were collected<sup>60</sup>. The absorbance intensity accounts for the perceived number of photons absorbed and the area under the emission curve provides the number of emitted photons. The advantage of the relative method is that the use of different solvents can be accounted for by incorporation of their refractive indices. It is important to choose a standard with similar spectral properties to the unknown, trying to match the absorbance and emission maximums if possible. Zinc phthalocyanine (ZnPc) was used as a standard because it is well characterized in several solvents and has absorption and emission maxima at 670 and 675nm respectively<sup>52, 60</sup>.

Distortions in this type of measurement can occur from error in the absorption intensity as well as if the fluorescence changes nonlinearly with concentration. The concentrations



of the samples should be such that the absorbance intensities are no higher than 0.05 absorbance units (ABU). When concentrations are maintained at and under recommended levels, this change can be assumed as linear. Low concentrations also help mitigate any filter effects seen which lower the perceived emission<sup>52</sup>.

The relative method uses the ratio of the integrated fluorescence intensities, which corresponds to the ratio of known quantum yield to unknown. Using a well-defined standard with a known quantum yield, the unknown quantum yield is easily found using the equation 2. There are a few assumptions made during this procedure. It is assumed that both samples are exposed to the same number of photons at the same excitation wavelength. In order to use this method, first the absorbance and fluorescence spectra of the unknown and standard samples are collected at a minimum of three different concentrations. Also a solvent background is collected and taken into account. The integrated fluorescence is then plotted against the absorbance, maintaining an intercept of one. The slope of this plot is then used to calculate the quantum yield<sup>52</sup>.

$$\Phi_x = \Phi_{St} \left( \frac{Grad_x}{Grad_{St}} \right) \left( \frac{\eta_x^2}{\eta_{St}^2} \right)$$

Equation 2: Relative quantum yield of an unknown ( $\Phi_x$ ) can be established through this equation using a well-established standard, where Grad is the slope of the integrated fluorescence intensity vs. the absorbance intensity and  $\eta$  is the refractive index.

Cross linker

The linker was prepared through a simple nucleophilic substitution between the halogen on the azidopropane species and the hydroxide group present in NHS. This reaction is commonly known as a Williamson ether synthesis and was done using simple reaction conditions in a carbonate buffer<sup>61</sup>. This gave a good efficiency of upwards of 60% yields. The yellow oil obtained was initially thought to be reactive with water, which would be problematic in the application of the probe, however testing in water verified that after a week no degradation of the initial compound was seen.

### Assembly of Probe

The reaction to assemble the probe was a common click reaction between azide and alkyne functionalities. As the final product was run through a column, it cannot truly be categorized as a click type reaction because click type reactions are characterized by simple methods of purification such as recrystallization or filtration<sup>27</sup>. However it is thought that this purification technique was not necessary. A way to remove excess copper (II) sulfate and sodium ascorbate needs to be determined. Usually washing with water is sufficient, however as the product is extremely water soluble, this was ineffective. It was thought that any unreacted materials would be cleaned through the final binding with the protein and subsequent dialysis. This prevents us from establishing an accurate yield, as unreacted species may still be present in the product solution, even after separation through the column. Establishing an effective means of product isolation would be of great interest to be able to report a reasonable yield. Due to the nature of the reaction and evidence of the formation of a 1, 2, 3 triazole shown in <sup>1</sup>H NMR binding did

occur. The hydrogen in the triazole ring was evident by a singlet 7.83 ppm and the signal at 2.75 ppm had a lower integration due to the disappearance of alkyne functionality.

Running the reaction at a slightly increased temperature as well as an increased time may help reduce the amount of unreacted species.

### Conjugation to a Protein

BSA was used as a model protein system to determine if the probe was sufficient for its intended application. This was done using common protein labeling techniques presented by Fisher Scientific. Dialysis was used on a micro scale to purify a small portion of the reaction solution. A mini dialysis tube was first soaked in PBS to remove any glycerin present. The mini tube had a high molecular weight cut off to ensure that any unreacted materials other than protein would be eliminated through osmosis. The purification was determined to be complete when no further loss of color was seen, at which point the PBS was changed one more time as a precaution. Successful binding was assumed through visual inspection, as the remaining BSA solution was blue in color, as well as through spectral methods. The absorbance and emission wavelength were identical to that of the free dye, with a slight loss in emission intensity seen between figure 14 and figure 17.

## CHAPTER FIVE

### CONCLUSION

The cyanine derivative with alkyne functionality was successfully synthesized with slight modification to the method outlined in Shao, et al.,<sup>1</sup>. It was shown that the NHS could be modified to contain an azidopropane moiety which allowed its participation in click type cycloadditions between azide and alkyne moieties. This click type reaction bound the dye successfully to the NHS derivative, allowing for lysine containing species to be labeled or targeted by the probe. BSA was used as a model system to determine if the NHS moiety would bind with protein without the presence of an NHS ester commonly used for protein labeling. After 3 days of dialysis, it was determined that binding did occur by visual inspection and spectral properties. Free dye and impurities smaller than 10,000 grams/mole were able to pass through the membrane while dye bound to protein remained.

## CHAPTER SIX

### FUTURE WORK

Using a model system, binding does appear to occur. However, future testing should be done. Binding should be verified through SDS-Page testing, a protein separation technique which would allow for the bound dye to be distinguished through a photo reactive band at the characteristic site of the protein. In addition to this, a more complete spectral analysis should be done, including the quantum yield and molar absorptivity. As this is only a model system, the molecular probe should also be tested against other proteins, such as human serum albumin, as well as specific proteins which are overexpressed on the surface of tumors.

Another avenue to pursue would be the synthesis of an ester type NHS derivative, which may be more reactive towards primary amides found in proteins. This reactivity would also be increased in water and may cause the probe to be unstable in aqueous solutions<sup>29</sup>.

Different means of binding could also be attempted through the direct modification of the dianil intermediate of the initial dye. By incorporating an NHS ester or maleimide on the site where the alkyne is attached a condensed method of targeting may be accomplished. This modification may come with modified spectral characteristics which should be considered and investigated.

One area that would be of great interest is the incorporation of a Förster resonance energy transfer (FRET) pair to increase the effective Stokes shift. A FRET paired dye absorbs at the emission wavelength of a mate, providing a means for a second absorption and emission phenomenon. This mechanism provides a means for longer emission wavelengths and an increase in the perceived Stokes shift, providing a better signal to noise ratio at increased depths. Although this seems easy to accomplish, the chromophores must be within 10nm of each other for FRET to occur. The determination and attachment of a FRET counter chromophore would present an entirely new project<sup>62</sup>.

## REFERENCES

1. Shao, F. W.; Weissleder, R.; Hilderbrand, S. A., Monofunctional Carbocyanine Dyes for Bio- and Bioorthogonal Conjugation. *Bioconjugate Chemistry* **2008**, *19* (12), 2487-2491.
2. Luo, S.; Zhang, E.; Su, Y.; Cheng, T.; Shi, C., A review of NIR dyes in cancer targeting and imaging. *Biomaterials* **2011**, *32* (29), 7127-7138.
3. Robbins, J. B.; Pozniak, M. A., Contrast Media Tutorial. University of Wisconsin Department of Radiology, 2010.
4. Becker, A.; Hossenius, C.; Licha, K.; Ebert, B.; Sukowski, U.; Semmler, W.; Wiedenmann, B.; Grotzinger, C., Receptor-targeted optical imaging of tumors with near-infrared fluorescent ligands. *Nat Biotechnol* **2001**, *19* (4), 327-31.
5. Kovar, J. L.; Simpson, M. A.; Schutz-Geschwender, A.; Olive, D. M., A systematic approach to the development of fluorescent contrast agents for optical imaging of mouse cancer models. *Biochemistry--Faculty Publications* **2007**, *9*.
6. Administration, T. U. S. F. a. D. Medical Imaging. <http://www.fda.gov/Radiation-EmittingProducts/RadiationEmittingProductsandProcedures/MedicalImaging/default.htm>.
7. Balas, C., Review of biomedical optical imaging—a powerful, non-invasive, non-ionizing technology for improving in vivo diagnosis. *Measurement Science and Technology* **2009**, *20*, 104020.
8. Robb, R. A.; Director, B. I. R., Biomedical imaging: Past, present and predictions. *Journal of Medical Imaging Technology* **2006**, *1*, 25-37.
9. Administration, T. U. S. F. a. D., Medical Imaging: Ultrasound Imaging. 2011.
10. Duck, F., Hazards, risks and safety of diagnostic ultrasound. *Medical Engineering & Physics* **2008**, *30* (10), 1338-1348.
11. Research, T. M. F. f. M. E. a. Ultrasound. <http://www.mayoclinic.com/health/ultrasound/MY00308>.
12. Paladini, D., Sonography in obese and overweight pregnant women: clinical, medicolegal and technical issues. *Ultrasound in Obstetrics and Gynecology* **2009**, *33* (6), 720-729.
13. Fred, H. L., Drawbacks and limitations of computed tomography: views from a medical educator. *Tex Heart Inst J* **2004**, *31* (4), 345-8.
14. Brenner, D. J.; Hall, E. J., Computed Tomography- An increasing source of radiation exposure. *New England Journal of Medicine*: 2007; Vol. 357, pp 2277-84.
15. Gauden, A. J.; Phal, P. M.; Drummond, K. J., MRI safety; nephrogenic systemic fibrosis and other risks. *Journal of Clinical Neuroscience* **2010**, *17* (9), 1097-1104.
16. Main, M. L., Ultrasound Contrast Agent Safety. *JACC: Cardiovascular Imaging* **2009**, *2* (9), 1057-1059.
17. Marshall, G.; Kasap, C., Adverse events caused by MRI contrast agents: Implications for radiographers who inject. *Radiography* **2010**.

18. Goldberg, B. B.; Liu, J.-B.; Forsberg, F., Ultrasound contrast agents: A review. *Ultrasound in Medicine & Biology* **1994**, *20* (4), 319-333.
19. Rundback, J. H.; Nahl, D.; Yoo, V., Contrast-induced nephropathy. *Journal of Vascular Surgery* **2011**, *54* (2), 575-579.
20. Kitajima, K.; Maeda, T.; Watanabe, S.; Sugimura, K., Recent issues in contrast-induced nephropathy. *International Journal of Urology* **2011**, *18* (10), 686-690.
21. Desmettre, T.; Devoisselle, J. M.; Mordon, S., Fluorescence properties and metabolic features of indocyanine green (ICG) as related to angiography. In *Surv Ophthalmol*, United States, 2000; Vol. 45, pp 15-27.
22. Weissleder, R.; Tung, C. H.; Mahmood, U.; Bogdanov, A., In vivo imaging of tumors with protease-activated near-infrared fluorescent probes. *Nature Biotechnology* **1999**, *17* (4), 375-378.
23. Bouteiller, C.; Clavé, G.; Bernardin, A.; Chipon, B.; Massonneau, M.; Renard, P.-Y.; Romieu, A., Novel Water-Soluble Near-Infrared Cyanine Dyes: Synthesis, Spectral Properties, and Use in the Preparation of Internally Quenched Fluorescent Probes. *Bioconjugate Chemistry* **2007**, *18* (4), 1303-1317.
24. Hilderbrand, S. A.; Kelly, K. A.; Weissleder, R.; Tung, C.-H., Monofunctional Near-Infrared Fluorochromes for Imaging Applications. *Bioconjugate Chemistry* **2005**, *16* (5), 1275-1281; Kulbacka, J., Cyanines as efficient photosensitizers in photodynamic reaction: Photophysical properties and in vitro photodynamic activity. Pola, A., Ed. Pleiades Publishing Ltd.: 2011; Vol. 76, pp 473-479.
25. Ye, Y. P.; Bloch, S.; Kao, J.; Achilefu, S., Multivalent carbocyanine molecular probes: Synthesis and applications. *Bioconjugate Chemistry* **2005**, *16* (1), 51-61.
26. INC, J. I. L. Technical Information on Probes Conjugated to Affinity-Purified Antibodies and to Other Proteins: Cyanine Dyes (Cy2, Cy3, and Cy5). <http://www.jacksonimmuno.com/technical/f-cy3-5.asp>.
27. Kolb, H. C.; Finn, M. G.; Sharpless, K. B., Click Chemistry: Diverse Chemical Function from a Few Good Reactions. *Angewandte Chemie International Edition* **2001**, *40* (11), 2004-2021.
28. Scientific, T. *Instructions: NHS-Fluorescein*; Thermo Fisher Scientific Inc: 2008; pp 1-4.
29. Lutz, J. F.; Borner, H. G., Modern trends in polymer bioconjugates design. *Progress in Polymer Science* **2008**, *33* (1), 1-39.
30. Weissleder, R.; Ntziachristos, V., Shedding light onto live molecular targets. *Nat Med* **2003**, *9* (1), 123-128.
31. Ziskin, M. C.; Petitti, D. B., Epidemiology of human exposure to ultrasound: A critical review. *Ultrasound in Medicine & Biology* **1988**, *14* (2), 91-96.
32. Letter, U. B. W., Do You Really Need That CT Scan? Berkley, U., Ed. Remedy Heath Media LLC: 2010; Vol. October.
33. Shellock, F. G., Magnetic resonance safety update 2002: implants and devices. *Journal of magnetic resonance imaging* **2002**, *16* (5), 485-496.
34. Nikken, J. J.; Krestin, G. P., MRI of the kidney—state of the art. *European Radiology* **2007**, *17* (11), 2780-2793.



35. Uppot, R. N.; Sahani, D. V.; Hahn, P. F.; Gervais, D.; Mueller, P. R., Impact of obesity on medical imaging and image-guided intervention. *American Journal of Roentgenology* **2007**, *188* (2), 433.
36. Chance, B.; Cope, M.; Gratton, E.; Ramanujam, N.; Tromberg, B., Phase measurement of light absorption and scatter in human tissue. *Review of scientific instruments* **1998**, *69*, 3457.
37. Dolan, M. S.; Gala, S. S.; Dodla, S.; Abdelmoneim, S. S.; Xie, F.; Cloutier, D.; Bierig, M.; Mulvagh, S. L.; Porter, T. R.; Labovitz, A. J., Safety and Efficacy of Commercially Available Ultrasound Contrast Agents for Rest and Stress Echocardiography. *Journal of the American College of Cardiology* **2009**, *53* (1), 32-38.
38. Meacock, L. M.; Sellars, M. E.; Sidhu, P. S., Microbubble agents help pinpoint renal lesions | Page 5 - Diagnostic Imaging. *Diagnostic Imaging Europe*: 2009; Vol. 25.
39. Hillman, E. M. C.; Moore, A., All-optical anatomical co-registration for molecular imaging of small animals using dynamic contrast. *Nat Photon* **2007**, *1* (9), 526-530.
40. Ripamonti, D.; Barbò, R.; Rizzi, M.; Finazzi, M. G.; Ravasio, L.; Bonaldi, G.; Suter, F., New Times for an Old Disease: Intracranial Mass Lesions Caused by Mycobacterium tuberculosis in 5 HIV-Negative African Immigrants. *Clinical Infectious Diseases* **2004**, *39* (5), e35-e45.
41. Taneja, A.; Reis, F.; Rogerio, F.; Queiroz, L.; Zanardi, V., *Meningeal presentation of an atypical teratoid/rhabdoid tumor*. 2010; Vol. 58, p 681-682.
42. Weissleder, R.; Mahmood, U., Molecular Imaging. *Radiology* **2001**, *219* (2), 316-333.
43. Terai, T.; Nagano, T., Fluorescent probes for bioimaging applications. *Current Opinion in Chemical Biology* **2008**, *12* (5), 515-521.
44. Hermanson, G. T., *Bioconjugate techniques*. Academic Press: 1996.
45. Rao, J.; Dragulescu-Andrasi, A.; Yao, H., Fluorescence imaging in vivo: recent advances. *Current opinion in biotechnology* **2007**, *18* (1), 17-25.
46. Frangioni, J. V., In vivo near-infrared fluorescence imaging. *Current Opinion in Chemical Biology* **2003**, *7* (5), 626-634.
47. Allison, R., Photosensitizers in clinical PDT. *Photodiagnosis and Photodynamic Therapy* **2004**, *1* (1), 27-42.
48. Juarranz, Á.; Jaén, P.; Sanz-Rodríguez, F.; Cuevas, J.; González, S., Photodynamic therapy of cancer. Basic principles and applications. *Clinical and Translational Oncology* **2008**, *10* (3), 148-154.
49. Oshiki, D.; Kojima, H.; Terai, T.; Arita, M.; Hanaoka, K.; Urano, Y.; Nagano, T., Development and Application of a Near-Infrared Fluorescence Probe for Oxidative Stress Based on Differential Reactivity of Linked Cyanine Dyes. *Journal of the American Chemical Society* **2010**, *132* (8), 2795-2801.
50. Lakowicz, J. R., *Principles of fluorescence spectroscopy*. Springer: New York, NY, 2006.
51. Fery-Forgues, S.; Lavabre, D., Are Fluorescence Quantum Yields So Tricky to Measure? A Demonstration Using Familiar Stationery Products. *Journal of Chemical Education* **1999**, *76* (9), 1260-null.

52. Horiba, J. Y., A Guide to Recording Fluorescence Quantum Yields.
53. Cheong, W. F.; Prahl, S. A.; Welch, A. J., A review of the optical properties of biological tissues. *Quantum Electronics, IEEE Journal of* **1990**, *26* (12), 2166-2185.
54. Bigio, I. J.; Mourant, J. R., Ultraviolet and visible spectroscopies for tissue diagnostics: fluorescence spectroscopy and elastic-scattering spectroscopy. *Physics in medicine and biology* **1997**, *42*, 803.
55. Mujumdar, S. R.; Mujumdar, R. B.; Grant, C. M.; Waggoner, A. S., Cyanine-Labeling Reagents: Sulfobenzindocyanine Succinimidyl Esters. *Bioconjugate Chemistry* **1996**, *7* (3), 356-362.
56. Kiernan, J., Classification and naming of dyes, stains and fluorochromes. *Biotechnic & histochemistry* **2001**, *76* (5-6), 261-278.
57. Chipon, B.; Clavé, G.; Bouteiller, C.; Massonneau, M.; Renard, P.-Y.; Romieu, A., Synthesis and post-synthetic derivatization of a cyanine-based amino acid. Application to the preparation of a novel water-soluble NIR dye. *Tetrahedron Letters* **2006**, *47* (47), 8279-8284; Jiang, L.-L.; Dou, L.-F.; Li, B.-L., An efficient approach to the synthesis of water-soluble cyanine dyes using poly(ethylene glycol) as a soluble support. *Tetrahedron Letters* **2007**, *48* (33), 5825-5829.
58. Shao, F.; Yuan, H.; Josephson, L.; Weissleder, R.; Hilderbrand, S. A., Facile synthesis of monofunctional pentamethine carbocyanine fluorophores. *Dyes and Pigments* **2011**, *90* (2), 119-122.
59. Hein, C. D.; Liu, X. M.; Wang, D., Click chemistry, a powerful tool for pharmaceutical sciences. *Pharmaceutical Research* **2008**, *25* (10), 2216-2230; Wangler, C.; Schirmacher, R.; Bartenstein, P.; Wangler, B., Click-Chemistry Reactions in Radiopharmaceutical Chemistry: Fast & Easy Introduction of Radiolabels into Biomolecules for In Vivo Imaging. *Current Medicinal Chemistry* **2010**, *17* (11), 1092-1116.
60. Nesterova, I. V.; Verdree, V. T.; Pakhomov, S.; Strickler, K. L.; Allen, M. W.; Hammer, R. P.; Soper, S. A., Metallo-phthalocyanine near-IR fluorophores: Oligonucleotide conjugates and their applications in PCR assays. *Bioconjugate Chemistry* **2007**, *18* (6), 2159-2168.
61. Wade, L. G., *Organic Chemistry*. Prentice Hall: 2009.
62. Wu, W.-B.; Wang, M.-L.; Sun, Y.-M.; Huang, W.; Cui, Y.-P.; Xu, C.-X., Fluorescent polystyrene microspheres with large Stokes shift by fluorescence resonance energy transfer. *Journal of Physics and Chemistry of Solids* **2008**, *69* (1), 76-82.